

# STRESS ANALYSIS OF A CONNECTING ROD

Thesis for the Degree of M. S.
MICHIGAN STATE COLLEGE
Elvin E. Tuttle
1954

3 1293 10395 9595

This is to certify that the

thesis entitled

STRESS ANALYSIS OF A

CONNECTING ROD

presented by

ELVIN E. TUTTLE

has been accepted towards fulfillment of the requirements for

M.S. degree in M.F.

Major professor

Date May 25 54



RETURNING MATERIALS:
Place in book drop to remove this checkout from your record. FINES will be charged if book is returned after the date stamped below.

1212-142

## STRESS ANALYSTS OF A CONNECTING ROD

By

Elvin E. Tuttle

## A THESIS

Submitted to the School of Graduate Studies of Michigan State College of Agriculture and Applied Science in partial fulfillment of the requirements for the degree of

MASTER OF SCIENCE

Department of Mechanical Engineering

#### ABSTRACT

A design for a one cylinder engine to be manufactured by the Michigan State College Mechanical Engineering Department has been developed by Dr. Louis L. Otto, Professor of Automotive Engineering. This thesis is the record of the experimental stress analysis to which the connecting rod for this engine was subjected.

The loads to which the connecting rod will be subjected in service were determined theoretically. This analysis involved assumptions of physical and operating characteristics and development of a pressure-volume diagram for the engine.

Using the previously developed theoretical loading, a theoretical stress analysis was made. To check these results, a sample connecting rod was cut from steel and statically tested using resistance wire strain gages. The sample connecting rod was also checked for stress concentrations, using the brittle lacquer coating method. Correlation between the experimental and theoretical stress analysis results was good.

The results of the theoretical stress analysis were plotted as a Soderberg diagram to illustrate the resistance of the connecting rod to repeated stresses. It was shown that a steel connecting rod of this design would be acceptable for use in the proposed engine. The Soderberg diagram also facilitates the checking of the suitability of other materials for use in the connecting rod.

Whipping stresses and their effect on the connecting rod stresses were also discussed. Assembly torque for the bearing cap holding screws was determined to prevent parting line separation.

#### ACKNOWLEDGMENTS

The author extends his sincere thanks to Dr. Louis L. Otto under whose supervision and guidance this analysis was made. He is also indebted to Professor Samuel Wercer, Jr. and the Applied Mechanics Department for the equipment used in the experimental analysis presented. The writer also wishes to thank Mr. Ray Pearson for advice and assistance in the manufacture of the sample connecting rod.

#### VITA

The author was born November 12, 1928 in the village of Pulaski, Jackson County, Michigan. He attended grade school in Hanover, Horton, and Pulaski, and graduated in May 1946 from Concord High School, valedictorian of his class.

In July 1946 he joined the United States Army. During the next thirty-five months he was stationed in Fort Belvoir, Virginia, San Jose Island in the bay of Panama, Fort Clayton, Canal Zone, St. Thomas, Virgin Islands, and Fort Riley, Kansas. During that time he was a stock record's clerk, responsible for maintaining records on both expendable and non-expendable property. For one year he was also manager of the Post Theater on San Jose Island. In June, 1949 he was discharged from the Army as a Sergeant (Grade III).

In September, 1949 he entered Michigan State College and in June, 1953 received a Bachelor of Science Degree in Mechanical Engineering. He was married in June, 1951. During the summers of 1952 and 1953 and part time during the school year 1952-53 he was employed as a Test Engineer at Reo Motors, Lansing. He is now a candidate for the degree of Master of Science in Mechanical Engineering.

He is a member of Tau Beta Pi, Pi Tau Sigma, Phi Kappa Phi, and Green Helmet.

## TABLE OF CONTENTS

I	Intro	ducti	.on	•	•	•	•	•	•	•	•	•	6
II	Proce	dure	•	•	•		•	•	•	•	•		9
	A.	Deve	lopr	nent	of	Conn	ecti	ng I	tod :	Loadi	.ng	•	9
	В.	Thec	ret	ical	Sti	ress .	Anal	ysis	·	•	•	•	2
	C.	Expe	erin:	enta.	l St	tress	Ana	lysi	ls.	•	•	•	3
III	Data	•	•	•	•	•	•	•	•	•	•	•	3.
IA	Discu	ssion	of	Data	а.	•	•	•	•	•	•	•	3!
V	Concl	usion	ıs	•	•	•	•	•	•	•	•	•	38
	Appen	dix	•	•	•	•	•	•	•	•	•	•	39
	A.	Whip	pine	g Stı	res	se <b>s</b>	•		•	•		•	39
	B.	Part	ing	Line	e Se	ep <b>ar</b> a	tion	•	•	•	•	•	40
	Bibli	og <b>ra</b> p	hy		•	•			•	•			4:

## TABLES

I	Development of Pressure-Volume Diagram	•	<b>1</b> 6
II	Crank Angles	•	13
III	Reciprocating-Inertia Forces	•	20
IA	Cosine of Angle Between Connecting Rod and Cylinder		
	Axis	•	20
V	Connecting Rod Loading	•	21-24
VI	Maximum and Minimum Connecting Rod Loads	•	26
VII	Experimental Data	•	33
VIII	Results of Experimental and Theoretical Stress		
	Analyses	•	34

## F1GURES

1.	Drawing of Proposed Connecting Rod Design	8
2.	Brake Mean Effective Pressure	10
3.	Mechanical Efficiency	11
4.	Engine Horsepower	13
5.	Pressure-Volume Diagram 4500 RPM Wide Open Throttle.	17
6.	Kinematic Sketch of Engine Movement	19
7.	Connecting Rod Loading 4500 RPM Wide Open Throttle .	25
8.	Cross Section of Connecting Rod	29
9.	Sample Connecting Rod	32
lo.	Development of Soderberg and Goodman Diagrams	35
11.	Soderberg Diagram of Connecting Rod Stresses	37
L2.	Parting Line Portion of Connecting Rod	40

#### I INTHODUCTION

In September of 1948 the Mechanical Engineering Department of Michigan State College inaugurated the manufacture of a small air compressor as the basis of several courses. The student followed this air compressor from the original casting of parts in the College Foundry through the final manufacture and assembly in the College Machine Shop. Advanced courses such as shop supervision, time study, and foundry research also used this air compressor as their base. After assembly the students were allowed to purchase the compressors for the cost of materials.

Soon the question arose as to whether a single cylinder engine would not be more popular than the air compressor with the students, thus generating more interest in the courses which were based upon it. An investigation by Dr. Louis L. Otto, Professor of Automotive Engineering at Michigan State College, produced a preliminary design for such an engine.

The object of this thesis is to determine, both analytically and experimentally, the stresses which will be encountered in the use of the connecting rod design suggested by Dr. Otto. The connecting rod as tested follows essentially the original design suggested by Dr. Otto, although some minor details were changed from the original design in the interest of easy manufacture.

The data pertaining to the engine design developed by Dr. Otto are as follows:

Bore - 2.5 inches

Stroke - 2.0 inches

Compression Ratio - 7.50 to 1

Brake Mean Effective Pressure - 50 psi at 4500 rpm

Mechanical Efficiency - approx. 50% at 4500 rpm

Estimated weight of reciprocating parts (Piston, Pin, Rings, Top

end of Rod, etc.) - 1.05 pounds

Weight of rotating end of rod - 0.8 pound

Engine type - Four-stroke cycle

A drawing of the connecting rod analyzed in this investigation is presented in Figure 1.

The bearing dimensions of the rod are those developed by Dr. Otto using accepted theoretical procedures and compare favorably with designs now being used in practice.

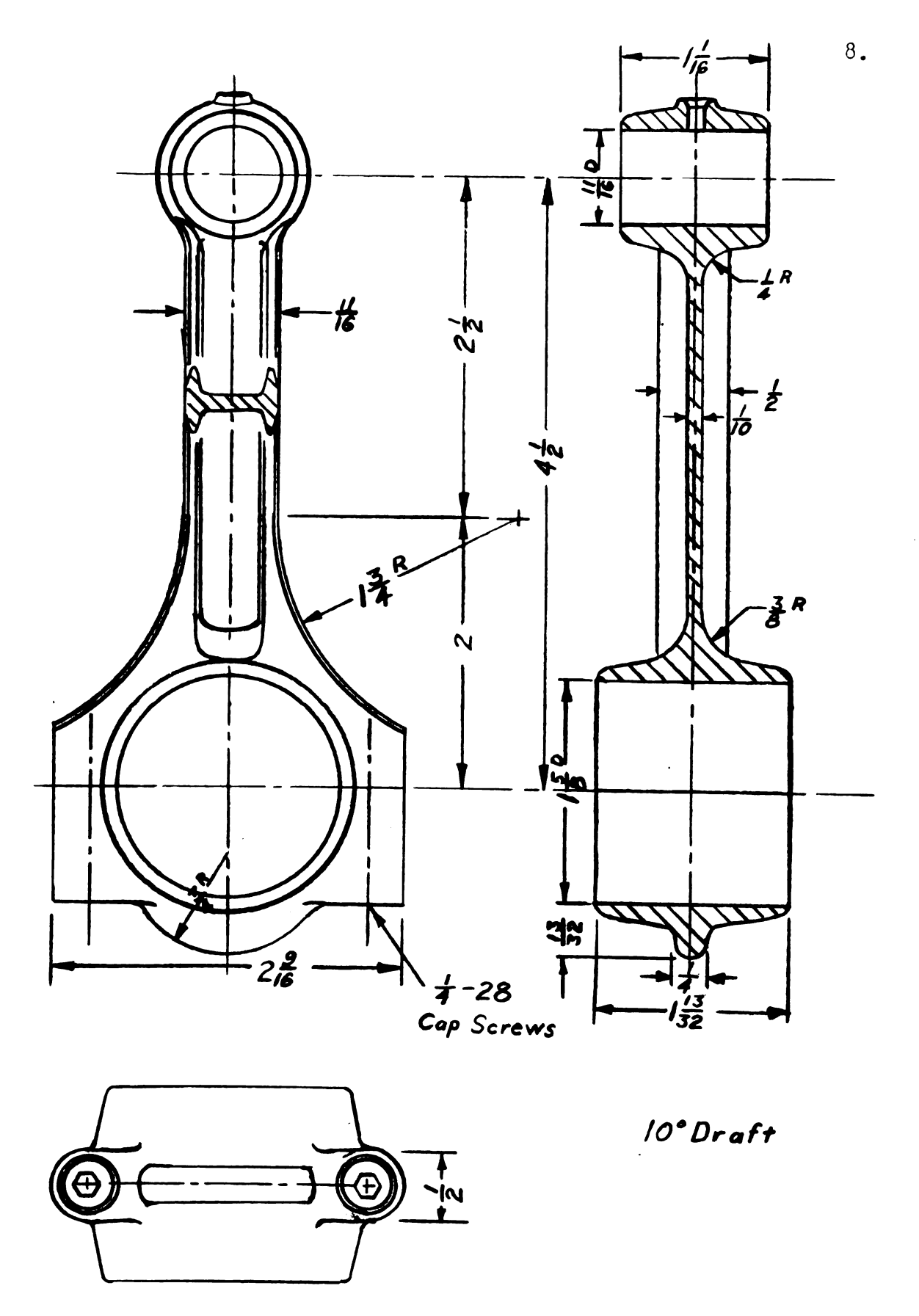


Fig. 1. Drawing of Proposed Connecting Rod Design

#### II PROCEDURE AND APPARATUS

## A. Development of Connecting Rod Loading

The investigation leading to the design of components of this engine required that values of Brake Mean Effective Pressure and Mechanical Efficiency be assumed over the speed range in which the engine will operate. Such assumptions are shown as curves in Figures 2 and 3. These curves have the same general shape as experimentally determined curves of actual engines. However, the exact determination of these characteristics must await the construction and testing of a sample engine.

The horsepower characteristics of the proposed engine were then determined using the equation<sup>2</sup> BHP =  $\frac{\text{PLAN}}{33,000}$  wherein:

BHP = Brake Horsepower

P = Brake mean effective pressure in psi

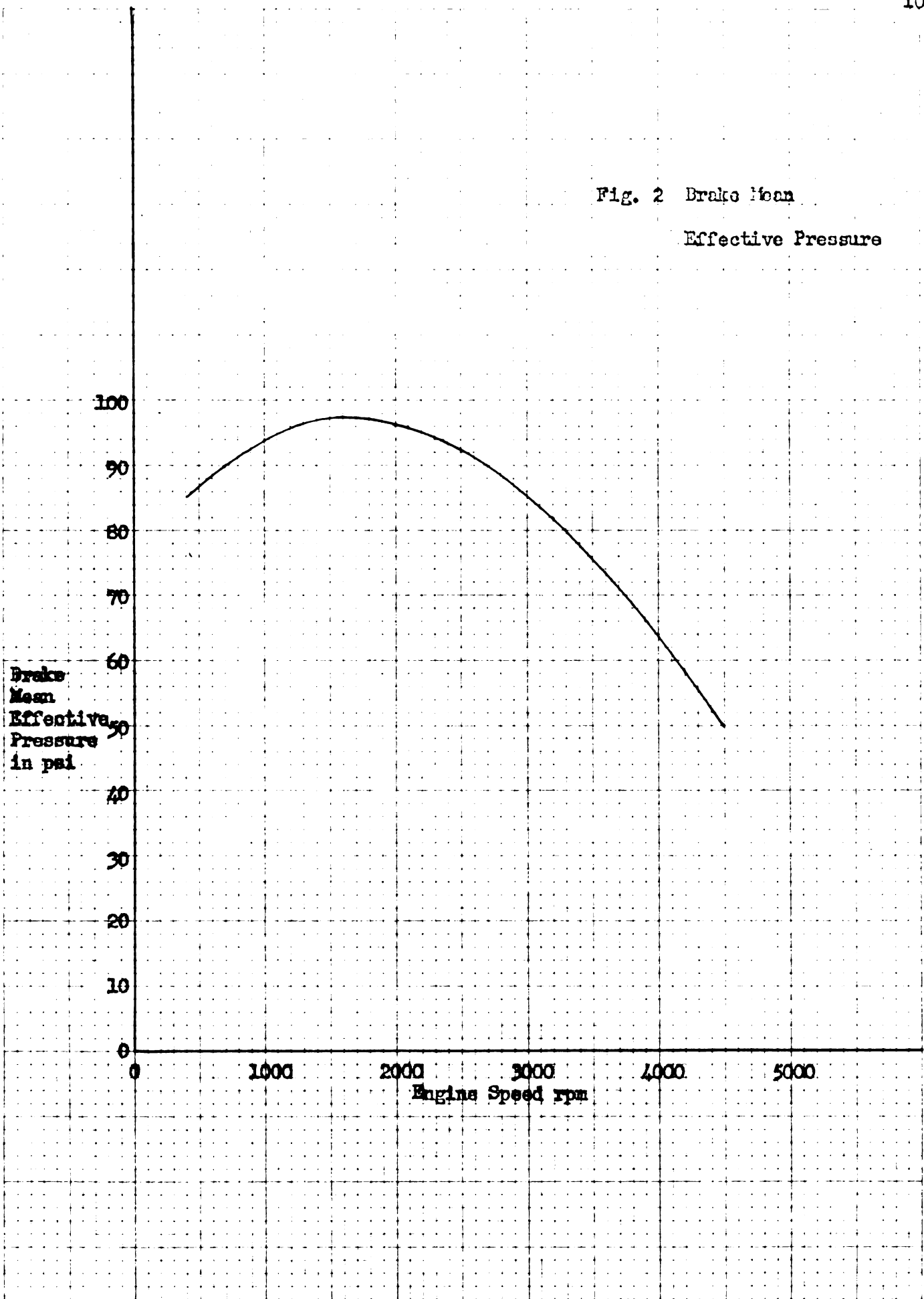
L = Length of stroke in feet

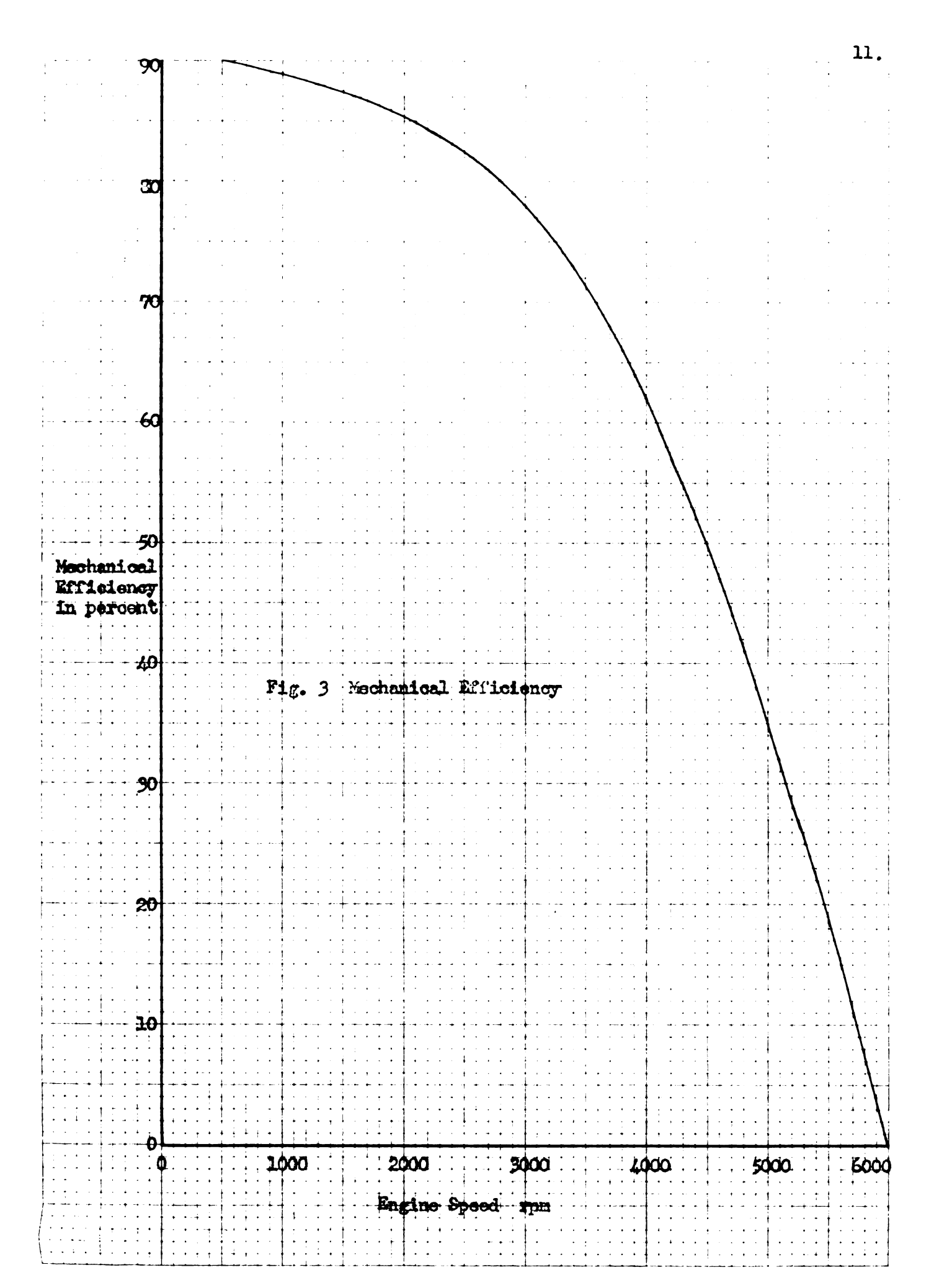
A = Projected area of piston crown in square inches

N = Number of power strokes per minute - in this case
half the number of revolutions per minute

For an example of performance curves for an engine of this type, see Virgil Moring Faires, Applied Thermodynamics, Revised Edition, The MacMillan Company, New York, Seventh Printing, 1950, p. 130

<sup>&</sup>lt;sup>2</sup>Ibid., p. 113





The results of this determination are shown in curve form in Figure 4.

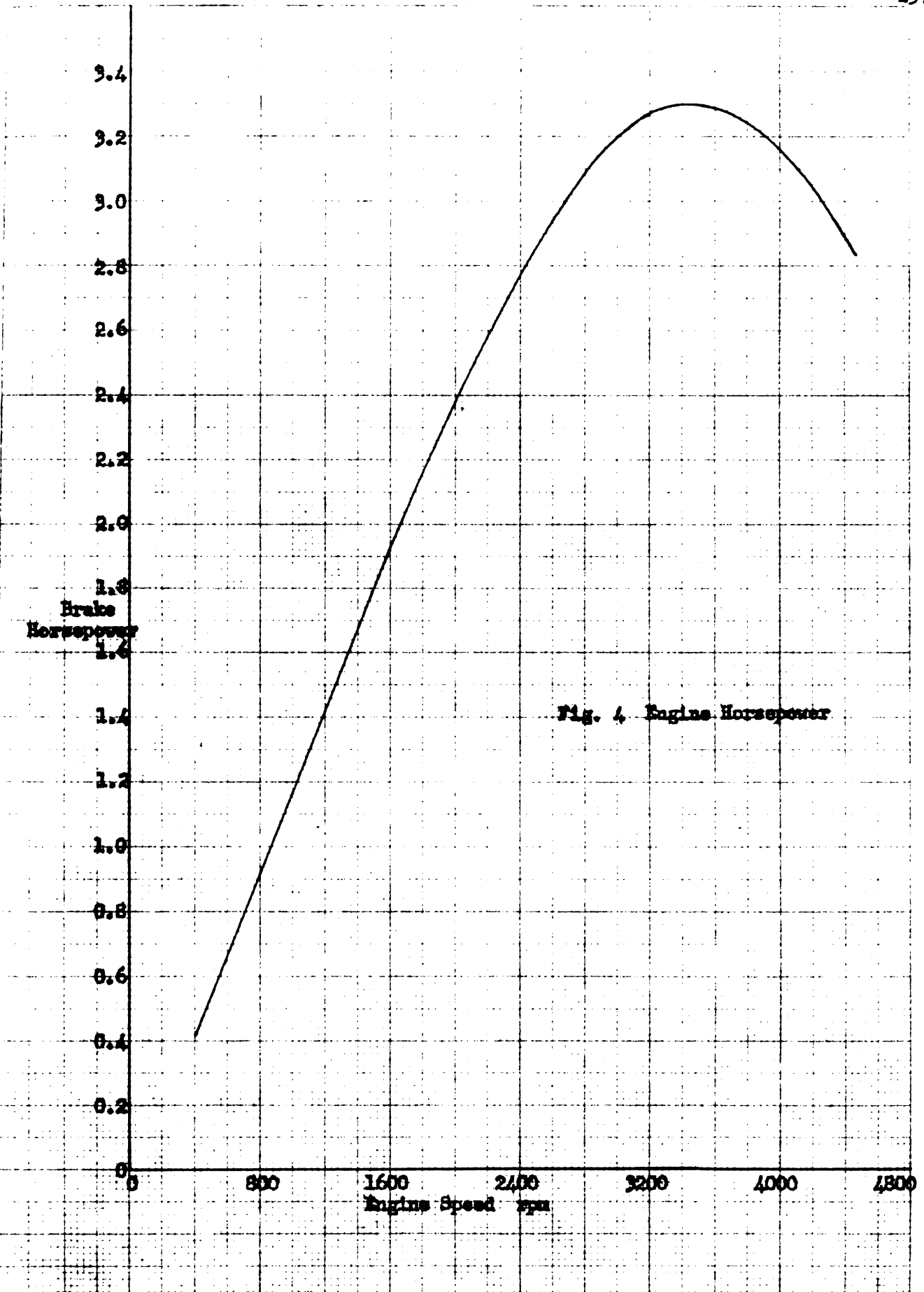
The next step in the determination of the connecting rod loading was the construction of a pressure volume diagram or indicator card.

This was done for wide open throttle operation at 4500 rpm as follows:

Let  $V_1$  be the volume of the cavity above the piston when the crankshaft is at bottom dead center and  $V_2$  be the volume of the cavity above the piston when the crankshaft is at top dead center. Taking volume as the abscissa and absolute pressure as the ordinate of the diagram, let  $V_1 - V_2 =$  one unit of volume. By definition  $V_1 = V_2$ . (Compression Ratio) = 7.5  $V_2$ . Substituting we have  $7.5V_2 - V_2 = 6.5V_2 =$  one unit of volume. Thus  $V_2 = 0.151$ 4 volume unit and  $V_1 = 1.151$ 4 volume units.

The displacement of the engine is the area of the top of the piston times the stroke and equals 9.81 cubic inches. The volume unit referred to above is equal to the engine displacement so one volume unit = 9.81 cubic inches. Then  $V_1 = 11.32$  cubic inches and  $V_2 = 1.51$  cubic inches.

In its idealized form the four-stroke cycle consists of a constant pressure intake stroke, a polytropic compression stroke, a constant volume energy addition, a polytropic expansion stroke and a constant pressure exhaust stroke. It was assumed that the engine is operating on an atmospheric pressure of 29.1 inches of mercury or 14.30 psi absolute (a reasonable average for the East Lansing area), and that at wide open throttle the intake vacuum is 1.5 inches of mercury or 0.74 psi. This yielded an intake line on the diagram at 13.56 psi absolute. The exhaust back pressure was assumed to be three inches of mercury or 1.48 psi.



Thus the exhaust line on the diagram lies at 15.78 psi absolute.

The compression and expansion strokes were assumed to follow the form  $PV^{n}$  = constant, where P is pressure and V is volume. For a realistic result, n was taken as approximately 1.3 for an engine using a mixture of air and gasoline vapor.<sup>3</sup>  $P_{1}$  and  $P_{2}$  are the pressures in the cylinder at the beginning and end respectively of the compression stroke in psi absolute and  $V_{1}$  and  $V_{2}$  have the meanings previously assigned. Then:

$$P_1 V_1^n = P_2 V_2^n$$

$$P_2 = P_1 (\frac{V_1}{V_2})^n \quad \text{but } \frac{V_1}{V_2} = \text{compression ratio}$$

so 
$$P_2 = P_1(\text{compression ratio})^n$$

The compression stroke was taken as starting at the end of the intake stroke ( $P_1$  = 13.56 psia) so  $P_2$  = 186.2 psi absolute. Intermediate pressures during the compression stroke were determined by taking appropriate values of compression ratio and solving as above.

To construct the pressure volume diagram, the brake mean effective pressures assumed earlier were converted to ideal indicated mean effective pressures. Actual Indicated Mean Effective Pressure = Brake Mean Effective Pressure x \_\_\_\_\_\_ . For 4500 RPM, where Mechanical Efficiency

Brake Mean Effective Pressure = 50 psia and Mechanical Efficiency = 50 percent the actual Indicated Mean Effective Pressure = 100 psi absolute.

The ideal Indicated Mean Effective Pressure desired is actual Indicated

<sup>3</sup>For a discussion of the choice of values of n, see Ibid., pp. 95-96

Mean Effective Pressure x card factor. This card factor compensates for losses at the beginning and end of the strokes due to the time necessary for burning of the air-fuel mixture and valve operation. Past experience has indicated that 1.07 is a reasonable value for card factor. Using this value, the ideal Indicated Mean Effective Pressure is 107 psi absolute. In one cycle this pressure does work by pushing on the piston crown and moving it through a distance equal to the stroke of the engine. Thus the work equivalent of the Indicated Mean Effective Pressure = (Ideal Indicated Mean Effective Pressure) x (Piston area) x (Stroke) = 87.5 foot pounds.

The work done by the compression stroke,  $\frac{1}{4} = \frac{\frac{P_2V_2 - P_1V_1}{1 - n}}{1 - n}$ .

The values previously obtained were substituted into this equation yielding  $_1W_2 = -35.6$  foot pounds. The negative sign indicates that work is done on the working fluid by the engine. Letting the work done on the engine by the working fluid after the constant volume energy addition (combustion), during the expansion stroke =  $_3W_4$  resulted in  $_3W_4 + _1W_2 = _3W_4$  work equivalent of Indicated Mean Effective Pressure. Thus  $_3W_4 = _3W_4 = _3W_4$  equivalent of Indicated Mean Effective Pressure =  $_1W_2 = _3V_3 = _3V_3 = _3V_3$ . foot pounds.

Let the ratio of  $3W_{1}/1W_{2} = R$ . Then R = 3.147. Since the work done on or by the engine is caused by and proportional to the pressure acting on the piston crown, the ratio of any pressure on the expansion stroke to the corresponding pressure on the compression stroke is also equal to R.

Using the above developments, Table I, evaluated for wide open throttle operation at 4500 RPM. is as follows:

<sup>4</sup>Tbid., p. 52

TABLE I

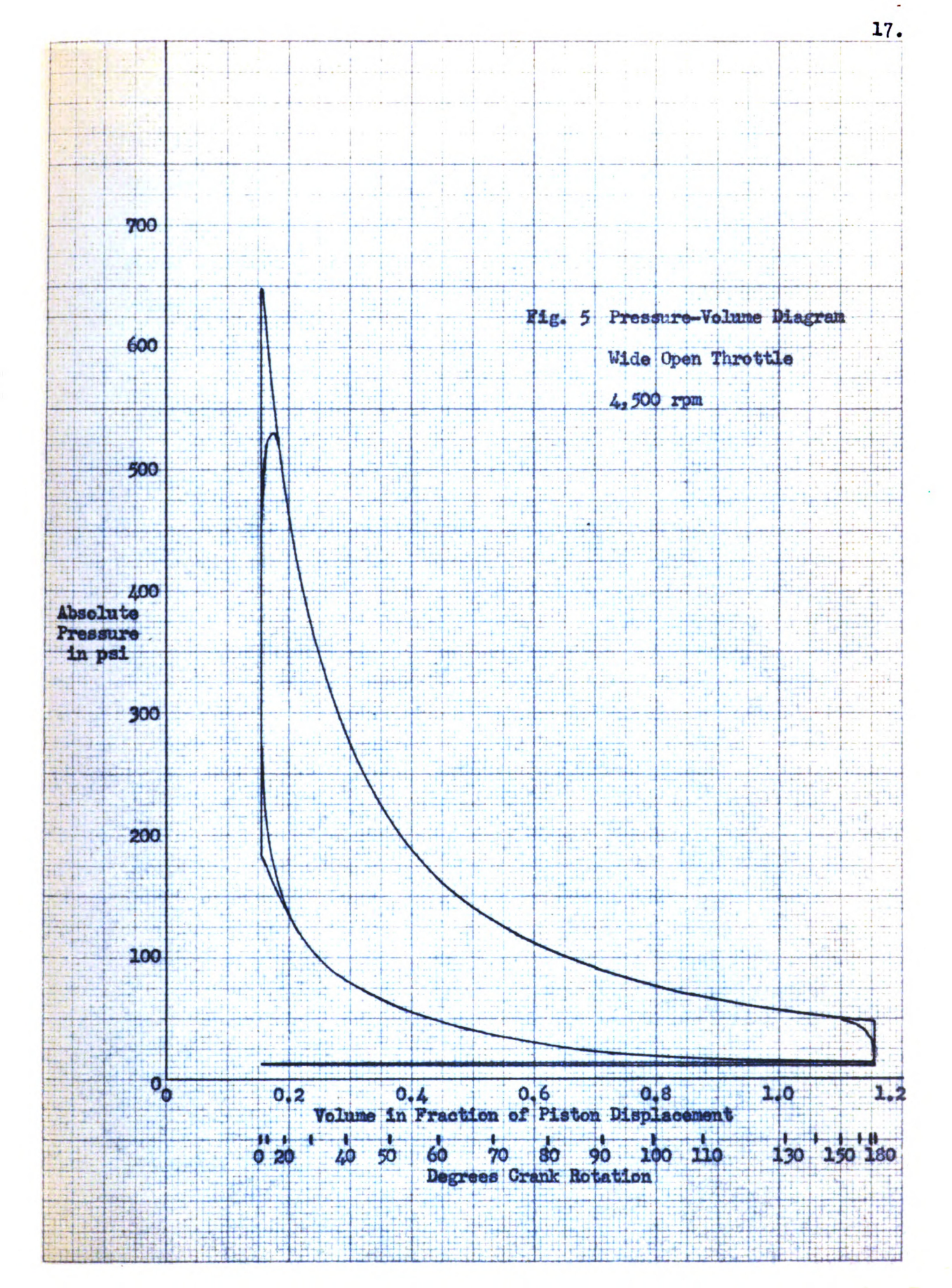
DEVELOPMENT OF PRESSURE-VOLUME DIAGRAM

Relative Volume in Decimal of Displacement	Ratio of Compression	(CR) <sup>1.3</sup>	Compression Pressure psi Absolute	Expansion Pressure psi Absolute
1.154	1	1	13.56	46.9
1.0	1.154	1.205	16.32	56 <b>.</b> 5
•9	1.283	1.382	18.73	64.9
.8	1.442	1.610	21.80	<b>75.</b> 5
•5	2.31	2.97	40.2	139.2
•3	3.85	5.76	78.1	270
.25	4.61	7.30	98.9	342
.2	5.77	9.77	132.3	458
.154	7.5	13.75	186.2	645

The complete pressure volume diagram is shown in Figure 5. To more nearly approximate an actual indicator card the corners have been rounded to take into account the time necessary for combustion and valve operation.<sup>5</sup>

Table II gives angle of crank rotation values from top dead center for corresponding volume values. This Table was used to place the crank angle scale on the pressure volume diagram and was developed as follows:

For illustrations of actual indicator cards see Ibid., p. 113;
Herman Diederichs and William C. Andrae, Experimental Mechanical
Engineering, Vol. I, John Wiley and Sons, New York, Seventh Printing,
1949, p. 306; Lester C. Lichty, Internal-Combustion Engines, Sixth
Edition, McGraw Hill, New York, 1951, p. 448



Partial Displacement Volume = percent piston travel x total displacement volume. When total displacement volume = one volume unit, as it does on Figure 5, partial displacement volume = percent piston travel expressed as a decimal. Then total volume = partial displacement volume plus clearance volume.

TAPLE II
CRANK ANGLES

Crank Angle in Degrees	% Piston Travel expressed as a Decimal	Clearance Volume	Total Volume
0	0.0	.154	.154
10	•009	.154	.163
20	.037	.154	.191
<b>3</b> 0	.081	.154	.235
40	.1ho	<b>.</b> 154	.291
50	.211	.15):	.365
60	.291	.154	.445
70	.378	.154	•532
80	.467	.154	.621
90	•556	.154	.710
100	.641	.154	•795
110	.720	.154	.874
120	.791	.154	.945
130	.854	.154	8oc.1
140	•906	.1514	1.060
150	·.947	.154	1.101
160	<b>.</b> 976	.154	1.130
170	•994	.1.54	1.1148
180	1.000	.154	1.154

<sup>6</sup>Lichty, op. cit., p. 482

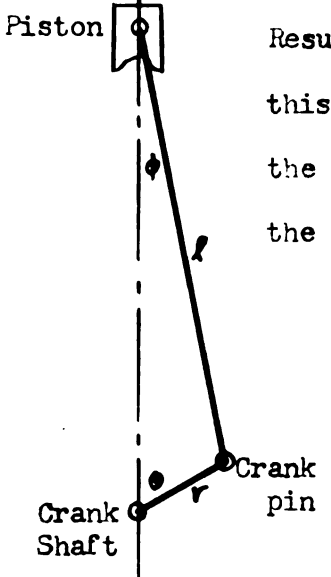
Determination of reciprocating inertia forces was made by evaluation of the equation  $F = 2.84 \times 10^{-5} \text{Mm}^2 \text{r} (\cos 9 + \frac{\text{r}}{\text{f}} \cos 2\theta)$  wherein

F = reciprocating inertia force in pounds

M = reciprocating weight in pounds

n = engine speed in rpm

r = crank radius in inches



## 0 = crank angle

Results of this evaluation are shown in Table III. In this Table it should be noted that forces acting toward the crankshaft are positive and forces acting away from the crankshaft are negative.

The total force acting on the piston crown is the effective gas pressure force (absolute pressure minus atmospheric pressure) in psi times the area of the piston crown. To this must be added the reciprocating inertia force. This

Fig. 6. Kinematic Sketch sum must be multiplied by the cosine of of Engine Movement the angle Ø between the connecting rod

and the cylinder axis to yield the axial connecting rod force. Evaluation of  $\emptyset$  for values of crank angle  $\Theta$  is given in Table IV where the symbols have the meanings shown in Figure 6.

$$\frac{\mathbf{r}}{\mathbf{l}} = \frac{\sin \emptyset}{\sin \theta} \qquad \qquad \sin \emptyset = \frac{\mathbf{r}}{\mathbf{l}} \sin \theta$$

$$\frac{\mathbf{r}}{\mathbf{l}} = .2222 \cdot \cdot \cdot \cdot \qquad \log \left(\frac{\mathbf{r}}{\mathbf{l}}\right) = 9.34674 - 10$$

<sup>7</sup>For the development of this equation, see Ibid., pp. 482-483

TABLE III
RECIPHOCATING INEATIA FORCES 4500 RPM

Crank Angle Degrees after Top Center	Acceleration Factor <sup>9</sup>	Reciprocating Inertia Force Pounds	Crank Angle Degrees after Top Center
0 10 20 30 40 50 60 70 80 90 100 110 120 130 140 150 160	-1.222 -1.194 -1.110977805604389172 .035 .222 .383 .512 .611 .682 .727 .755 .770 .776	-741 -725 -673 -593 -489 -366 -236 -104.3 8.49 134.3 232 310 372 415 4415 4411 459 467 471	360 350 340 330 320 310 300 290 280 270 260 250 240 230 220 210 200
180	<b>.</b> 778	472 	180 

TABLE IV

COSINE OF ANGLE BETWEEN CONNECTING ROD AND CYLINDER AXIS

Crank Angles	log(sin 0)	$\log(\frac{\mathbf{r}}{\mathbf{f}}\sin\theta) = \log(\sin\theta)$	log(cos Ø)	cos Ø
0 - 180 10 - 170 20 - 160 30 - 150 40 - 140 50 - 130 60 - 120 70 - 110 80 - 100 90	9.23967 9.53405 9.69897 9.80807 9.88425 9.93753 9.97299 9.99335	- 8.58641 8.88079 9.04571 9.15481 9.23099 9.28427 9.31973 9.34009 9.34674	9.99967 9.99875 9.99730 9.99552 9.99362 9.99180 9.99032 9.98936	1.0000 .9992 .9971 .9938 .9897 .9854 .9813 .9780 .9758

<sup>&</sup>lt;sup>8</sup>Ibid., p. 483

Table V and Figure 7 show the connecting rod loading for one cycle of wide open throttle operation of the engine at 4500 RPM.

TABLE V

CONNECTING ROD LOADING 4500 RPM
WIDE OPEN THROTTLE

A. Expansion Stroke

Crank Angle ATC <b>9°</b>	Effective Gas Pressure PSI Gage	Gas Pressure Force, #	Reciprocating Inertia Force, #	RIF + GPF #	Axial Rod Force #
0	328	1,612	-741	871	871
10	471	2,320	<b>-</b> 725	1,595	1,597
20	<b>4</b> 58	2,250	<b>-</b> 673	1,577	1,581
30	354	1,741	<b>-</b> 59 <b>3</b>	1,148	1 <b>,1</b> 56
40	<b>2</b> 62	1,289	<b>-</b> 489	800	809
50	199	9 <b>7</b> 9	<b>-</b> 366	613	629
60	1149	733	<b>-</b> 236	497	506
<b>7</b> 0	112	550	-104.3	445.7	456
80	89	437	8.49	445.49	456
90	<b>7</b> 3	<b>3</b> 69	134.3	503.3	516
100	62	<b>3</b> 05	232	537	550
110	53	261	310	571	<b>5</b> 85
120	47	231	372	603	6 <b>1</b> 14
130	42	207	415	622	631
140	<b>3</b> 8	187	441	<b>62</b> 8	645
150	34	167	459	626	631
<b>1</b> 60	28	138	467	605	606
170	17	83.5	471	554.5	555
180	7	34.4	472	506.4	506

TABLE V (cont.)

B. Exhaust Stroke

Crank Angle ATC	Effective Gas Pressure PSI Gage	Gas Pressure Force, #	Reciprocating Inertia Force, #	RIF + GPF #	Axial Rod Force #
190	2.5	12.3	471	483.3	484
200	1.5	7.37	467	474.37	475
210	1.5	7.37	459	466.37	470
220	1.5	7.37	441	448.37	453
230	1.5	7.37	415	422.37	429
240	1.5	7.37	372	379.37	386
250	1.5	7.37	310	317.37	324
<b>2</b> 60	1.5	7.37	232	239.37	245
270	1.5	7.37	134.3	141.67	145.1
<b>2</b> 80	1.5	7.37	8.49	15.86	16.23
<b>2</b> 90	1.5	7.37	-104.3	-96.93	<b>-</b> 99 <b>.</b> 0
300	1.5	7.37	<b>-23</b> 6	<b>-228.63</b>	<b>-</b> 233
310	1.5	7.37	<b>-</b> 366	-358.63	<b>-</b> 362
<b>3</b> 20	1.5	7.37	<b>-</b> 489	<b>-</b> 481.63	<b>-</b> 487
330	1.5	7.37	<b>-</b> 593	<b>-</b> 585 <b>.</b> 63	<b>-</b> 590
340	1.0	4.9	<b>-</b> 673	-668.1	<b>-</b> 670
350	<b>.</b> 5	2.46	<del>-</del> 725	-722.54	<b>-</b> 723
<b>3</b> 60	0	0	-741	-7,41	-741

TABLE V (cont.)

## C. Intake Stroke

Crank Angle ATC	Effective Gas Pressure Force #	Gas Pressure Force, #	Reciprocating Inertia Force, #	RIF + GPF #	Axial Rod Force #
370	0	0	<b>-7</b> 25	<del>-</del> 725	<b>-</b> 725
380	4	<b>-1.</b> 97	<b>-</b> 673	-674.97	<b>-</b> 676
<b>3</b> 90	8	-3.94	<b>-</b> 59 <b>3</b>	<b>-</b> 596 <b>.</b> 94	<b>-</b> 601
400	<b>-1</b>	-4.9	<b>-</b> 489	-493.9	<b>-</b> 499
410	-1	-4.9	<b>-3</b> 66	<b>-370.</b> 9	<b>-</b> 376
420	-1	-4.9	<b>-</b> 2 <b>3</b> 6	-240.9	<b>-</b> 246
430	-1	-4.9	-104.3	-109.2	-111.8
7770	-1	-4.9	8.49	<b>3.</b> 59	3.68
450	-1	-4.9	134.3	129.4	132.8
460	-1	-4.9	232	227.1	232
470	-1	-4.9	310	305.1	312
1,80	-1	-4.9	<b>3</b> 72	367.1	374
490	-1	-4.9	415	410.1	416
500	-1	-4.9	441	436.1	441
510	-1	-4.9	459	454.1	457
520	<b>-</b> 1	-4.9	467	462.1	464
530	-1	-4.9	471	466.1	467
540	-1	-4.9	472	467.1	467

TABLE V (cont.)

D. Compression Stroke

Crank Angle ATC <b>9°</b>	Effective Gas Pressure Force, #	Gas Pressure Force, #	keciprocating Inertia Force, #	RIF + GPF #	Axial Rod Force #
550	-1	-4.9	471	466.1	467
560	-1	-4.9	467	462.1	464
570	0	0	459	459	461
580	1	4.9	441	445.9	451
590	1.5	7.37	415	422.37	429
600	3	14.8	372	<b>3</b> 86.8	394
610	5	24.6	310	334.6	342
620	8	39.4	232	271.4	<b>27</b> 8
630	11	54.1	134.3	188.4	193.2
640	15	73.7	8.49	82.19	84.2
65 <b>0</b>	22	108.2	-104.3	3.9	4.0
660	33	162.2	<b>-2</b> 36	<b>-73.</b> 8	<b>-</b> 75 <b>.</b> 1
670	47	231	<b>-</b> 366	-135	-138.3
680	65	320	<b>-</b> 489 ·	<b>-1</b> 69	<b>-1</b> 70.9
690	91	447	<b>-</b> 59 <b>3</b>	-146	-147
<b>7</b> 00	133	654	<b>-</b> 673	<b>- 1</b> 9	- 19.06
710	21)4	1,052	<b>-7</b> 25	327	327

The above series of calculations was repeated to determine the maximum and minimum loading for wide open throttle operation at 200 RPm intervals from 400 to 4500 RPm.

TABLE VI

MAXIMUM AND MINIMUM CONNECTING ROD LOADS

Engine Speed	Maximum	Minimum
RPM	Load Pounds	Load Pounds
400	2,220	<b>-</b> 8.65
600	2 <b>,</b> 290	-14.51
800	2,339	<b>-</b> 23 <b>.</b> 26
1,000	2,381	<b>-36.</b> 5
1,200	2,405	<b>-</b> 52 <b>.</b> 6
1,400	2,417	-71.6
1,600	2,416	<b>-</b> 93 <b>.</b> 6
1,800	2,416	<b>-1</b> 18.3
2,000	2 <b>,3</b> 89	-146.1
2,200	2,359	<b>-176.</b> 8
2,400	2,316	-210
2,600	2,265	<del>-</del> 248
2,800	2,217	<b>-2</b> 86
3,000	2,145	<b>-</b> 339
3,200	2,076	-374
3,400	2,005	-421
3,600	1,939	-474
3,800	1,871	<b>-</b> 528
4,000	1,790	<b>-</b> 585
4,200	1,716	<b>-</b> 645
4,400	1,635	<b>-7</b> 08
4,500	1,597	-741
4,500*	479	<b>-</b> 773 <b>.</b> 2

<sup>\*</sup> Loading was also calculated for closed throttle operation at 4500 RPM. It was assumed in this case that, on the pressure volume diagram, the compression and expansion lines were identical.

## B. Theoretical Stress analysis

Determination of tension stresses in the connecting rod involved simply dividing the axial tensile load by the cross sectional area of the rod; s = P/A where s = stress in psi, P = load in pounds and A = cross sectional area of the rod. It must be remembered that, as developed above, negative forces produce tensile, or positive, stresses.

In determining compressive stresses the column effect was considered. For a short column hankine's column formula applies;

$$s = \frac{P}{A} [1 + K (\frac{P^2}{A^2})]$$

where  $\ell$  is column length, in inches,  $\rho$  is radius of gyration in inches, and K is a coefficient having a value of 0.4 x 10<sup>-14</sup> for a fixed end column and 1.6 x 10<sup>-14</sup> for a pin end column.

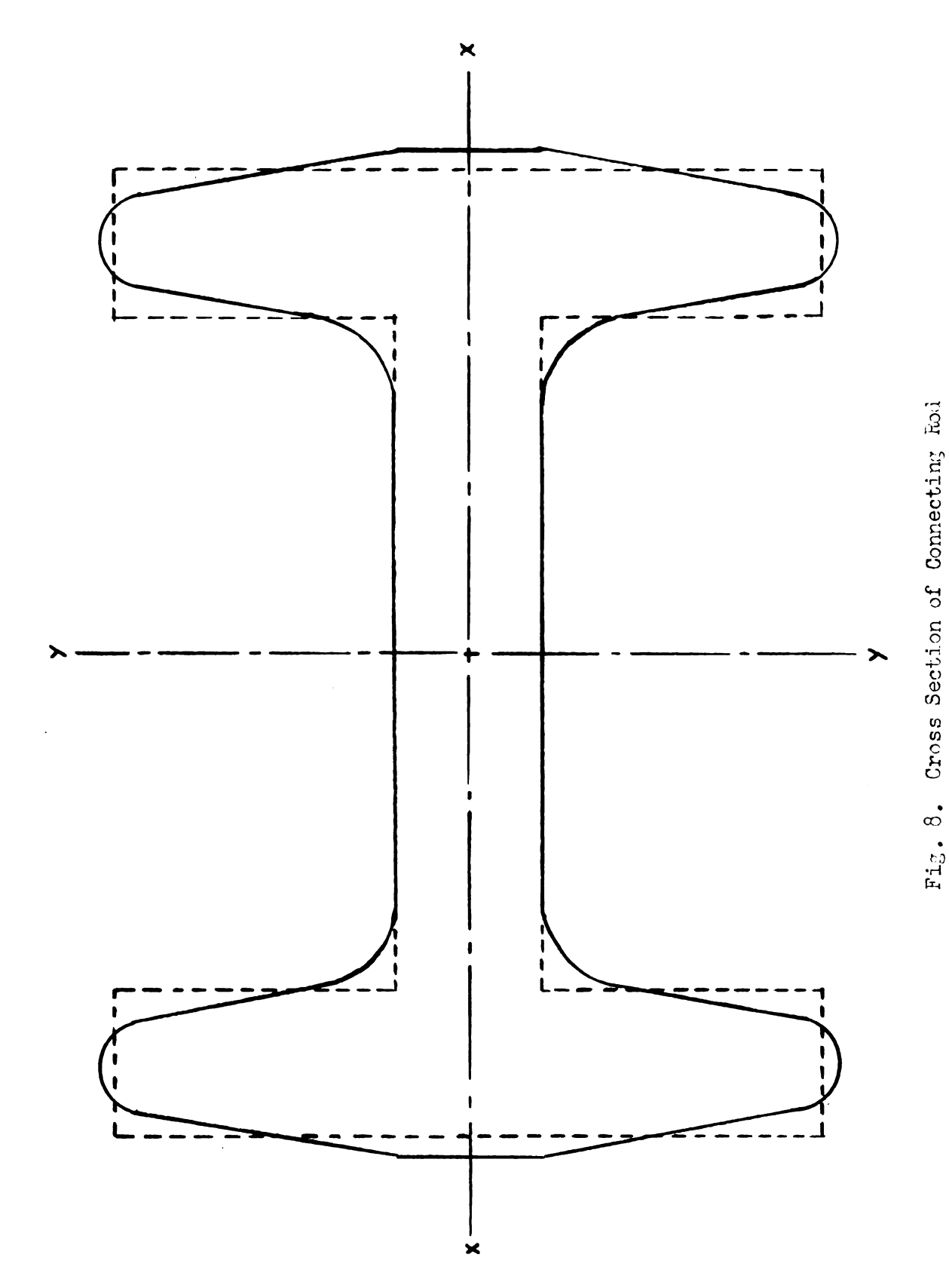
An enlarged scale drawing was made of the cross section of the connecting rod and is shown in Figure 8. To facilitate determination of radius of gyration the area outlined with dotted lines was used in calculations. Using the composite area method the moment of inertia about the x axis, I<sub>x</sub>, was determined to be 0.001dd2 in. 4 and the moment of inertia about the y axis, I<sub>y</sub>, was determined to be 0.003443 in. 4. The area of the dotted figure is 0.142 in. 2. It is interesting to note here that the actual cross sectional area of the rod is 0.139 in. 2 an error

<sup>&</sup>lt;sup>9</sup>Lionel S. Marks, <u>Mechanical Engineers' Handbook</u>, Fifth Edition, McGraw-Hill, New York, Third Impression, 1951, p. 466

<sup>10</sup>Charles O. Harris, Elementary Engineering Mechanics, Irwin-Farnham, Chicago, 1947, p. 200

of less than two percent. Continuing,  $\rho_X^2$  was evaluated as 0.01327 m<sup>2</sup> and  $\rho_Y^2$  was evaluated as 0.0593 in.<sup>2</sup> by use of the relation  $\rho^2 = \frac{f}{A}$ . About the x axis the connecting rod acts as a fixed end column and, when appropriate substitutions are made in the hankine formula, it was found that  $s = (1.0611)\frac{P}{A}$ . About the y axis the connecting rod acts as a pin end column and, when appropriate substitutions were egain made, it was found that  $s = (1.0546)\frac{P}{A}$ . Thus it may be seen that the higher compressive stresses result from column action producing bending in a plane parallel to the axis of rotation of the crankshaft. Thus highest compressive stresses may be anticipated on the edge of the flange of the "I" section of the rod. It should be noted again that positive loads as developed above produce compressive, or negative, stresses.

Whipping stresses are considered separately in a section of the Appendix.



Scale  $l^n = 0.1^n$ 

## C. Experimental Stress Analysis

To check the validity of the theoretical stress analysis, a sample connecting rod was made and tested by the author. This sample rod was machined from a bar of Halvan W4396 steel. A photograph of the completed rod is shown as Figure 9.

The sample connecting rod was checked for stress concentrations by coating with "Stresscoat" and applying the static loads previously calculated. The loading was done in an Olsen Testing machine located in the Heat Treat Laboratory at Michigan State College. "Stresscoat" is the trade name of a brittle lacquer coating manufactured by the Magnaflux Corporation in Detroit. When the material on which this brittle lacquer is sprayed undergoes strain, the lacquer cracks in a direction perpendicular to the strain. The spacing of these cracks indicates the magnitude of strain and consequently the stress.

It was found that, under the maximum compression load, a tension stress of approximately 30,000 psi occurred on the top edges of the crank bearing boss. This stress is due to the "wrapping" action of the bearing boss around the crank pin. This would indicate that close tolerances must be maintained in the manufacture of the engine parts to prevent "wrapping" action.

A resistance wire strain gage was then mounted on the edge of one flange in the middle of the I-beam section of the connecting rod. The rod was then statically loaded as before. The gage used was an SK-4 type A-19 manufactured by the Faldwin-Lima-Hamilton Corporation of Philadelphia. This gage had a resistance of 61 ohms and a gage factor of 1.61. The resistance wire strain gage measures the strain of the

material on which it is cemented by measuring the change in resistance of a tiny wire grid due to the dimensional change of the stretching wire. In this case the resistance change of the gage was measured by use of a Wheatstone bridge contained in an Anderson Strain meter. This instrument reads directly in micro-inches per inch strain and is calibrated for use with a 120 ohm gage with a gage factor of 2.05. Thus, to convert to actual strain the readings were multiplied by a resistance correction factor of  $\frac{120}{61}$  and a gage factor correction of  $\frac{1.61}{2.05}$ .

The true stresses were then calculated by multiplying the strains determined above by the modulus of elasticity of steel, 29,000,000 psi.

<sup>11</sup> Marks, op. cit., p. 398



Fig. 9 Sample Connecting Rod

### III DATA

Data obtained from the experimental stress analysis is given in Table VII. From this data empirical equations for tension stresses and

TABLE VII

EXPERIMENTAL DATA

Load in Pounds	Strain Reading in \(\mu\) in./in.	Actual strain in $\mu$ in./in	Stress in psi
774	114	176	5100
422	63	97	2820
0	0	0	О
<b>-1</b> 790	<b>-2</b> 85	-1410	<b>-12,</b> 780
-2417	<b>-3</b> 95	-610	<b>-17,7</b> 00

compression stresses in terms of load were evolved. For tension, s = 6.62P. For compression s = 7.25P. In both equations s is stress in psi and P is load in pounds. These equations are only approximate but match the observed values with a maximum error of 1.56 percent.

Table VIII is a tabulation of the maximum tension and compression stresses in the connecting rod over the operating speed range of the engine. The experimental results are computed using the empirical equations developed above.

TABLE VIII

RESULTS OF THEORETICAL AND EXPERIMENTAL

STRESS ANALYSES

Engine	Max. Tension Stress, psi		Max. Compression Stress, psi		
Speed RPM	Theoretical	Experimental	Theoretical	Experimental	
400	62.0	57.3	16,910	16,100	
60 <b>0</b>	104.1	96.1	17,460	16,600	
800	167	154	17,810	16,930	
1,000	254.5	242	18,170	17,280	
1,200	378	348	18,350	17,440	
1,400	5 <b>1</b> 4	474	18,400	17,500	
1,600	671	620	18,395	17,490	
1,800	849	784	18,390	17,490	
2,000	1,049	968	18,210	17,320	
2,200	1,268	1,170	17,980	17,100	
2,400	1,507	1,390	17,630	16,780	
2,600	1,780	1,642	17,300	16,420	
2,800	2,050	1,892	16,890	16,070	
3,000	2,430	2,240	16,370	15,580	
3,200	2,680	2,480	15,800	15,020	
3,400	3,030	2,790	15,300	14,550	
3,600	3,400	3,140	14,780	14,040	
3,800	<b>3,7</b> 85	3,500	14,280	<b>13,</b> 580	
4,000	4,200	3,870	13,640	12,990	
4,200	4,625	4,270	13,080	12,420	
4,400	5 <b>,</b> 080	4,690	12,470	12,850	
4,500	5,310	4,910	12,180	11,580	
4,500*	5,550	5,110	3,650	3,470	

<sup>\*</sup> Closed throttle

It should be noted that correlation between theoretical and experimental results was good, thus confirming the theoretical stress analysis.

### IV DISCUSSION OF DATA

The treatment of stresses of the nature developed in this connecting rod must include some means of taking into account the reaction of the material to repeated load. Such treatments are the use of the Goodman or the Soderberg theories. Assume a loading which produces a stress pattern similar to that shown in Figure 10(a). Let  $s_e$  be the endurance limit,  $s_u$  be the ultimate strength, and  $s_p$  be the elastic strength of the material. Then, according to the Goodman theory

$$\frac{s_r}{s_e} = 1 - \frac{s_a}{s_u}$$
, and according to the Soderberg theory  $\frac{s_r}{s_e} = 1 - \frac{s_a}{s_p}$ .

These relationships are best shown on a diagram such as Figure 10(b).

According to theory, if the point resulting from plotting the stress con-

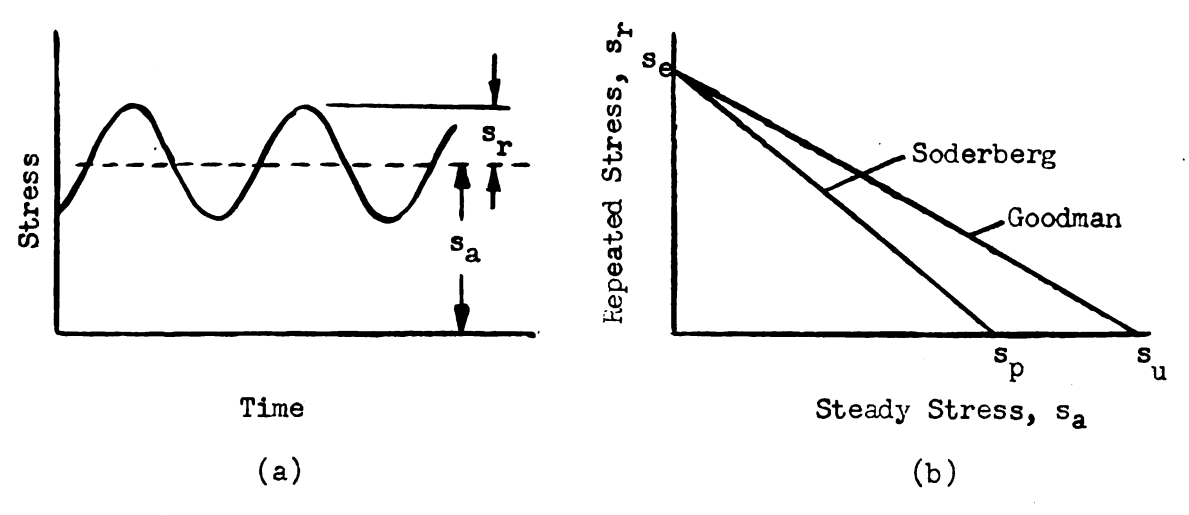


Fig. 10. Development of Soderberg and Goodman Diagrams

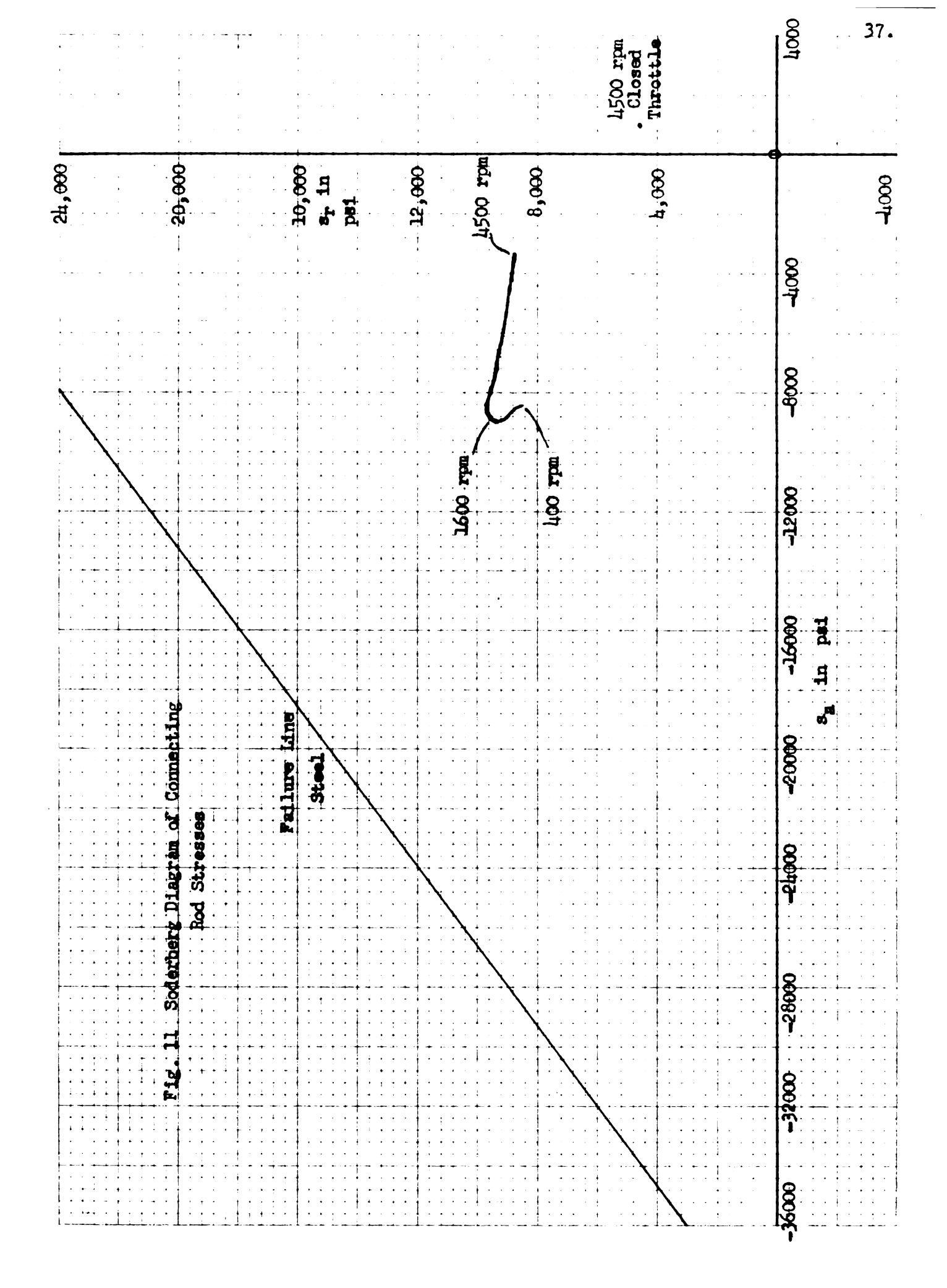
<sup>12</sup>The Goodman and Soderberg theories and Figure 8 are taken from Glenn Murphy, Advanced Mechanics of Materials, McGraw-Hill, New York, 1946, pp. 9-10

ditions on such a diagram lies outside the line, failure will occur.

It may be seen that the Soderberg theory is the more conservative of the two.

In applying these theories to engineering problems it is common to assume that the reversed loading applied to the member is approximated by a sine function having the same maximum and minimum values. This was done for the theoretical data and the results are shown as a Soderberg diagram as Figure 11. The theoretical stresses were used in this case since, as shown in Table VIII, they are at all speeds slightly more severe than the experimental stresses. Also included on the diagram is the failure line for a steel with a yield point of 40,000 psi and an endurance limit of 30,000 psi. These values are ultraconservative and could easily be exceeded in a machine steel properly heat treated or in other commonly used engineering materials such as aluminum or malleable iron.

The most critical engine speed range for connecting rod failure is 1,400 to 2,000 RPM wide open throttle.



## V CONCLUSIONS

The foregoing theoretical stress analysis and confirming experimental stress analysis indicate that the connecting rod design tested is entirely satisfactory and will operate in the engine under the most extreme conditions with a suitable margin of safety if steel is used as the rod material. If other materials are used, the Soderberg diagram in Figure 11 provides a convenient means to judge their suitability.

### APPENDIX

## A. Whipping Stresses

In addition to the stresses imposed on the connecting rod by the direct axial forces, whipping stresses were investigated. The maximum whipping stress is developed at the time when the connecting rod is at right angles with the crank throw and may be found by the Bach 13 formula:

$$s_b = 2 \times 10^{-6} n^2 r Ad / 2^2 / 2$$

sh = whipping stress in psi

where n = engine speed in rpm

r = crank radius in inches

A = cross sectional area of the rod in square inches

d = specific weight of rod material in pounds per cubic inch

length of connecting rod in inches

 $Z = section modulus in inches^3$ 

The above equation indicates that  $s_b$  varies as  $n^2$  so it was only necessary to consider high speed operation. Assuming a material of specific weight 0.28 pounds per cubic inch and an engine speed of 4,500 RPM, the whipping stress was evaluated to be 1,318 psi. Since the maximum stresses considered in this paper occur when the connecting rod is vertical and since the magnitude of the whipping stress is relatively small, the whipping stress is neglected in the stress analysis.

<sup>13</sup>Lichty, p. 553

## B. Parting Line Separation

As the cap screw holding the bearing cap onto the connecting rod is tightened the surface of the bearing cap is forced against the mating surface on the connecting rod. See Figure 12. This causes compression stresses to be set up in both the cap and the rod.

If the tensile force T is great enough to cause the cap and rod to separate, we have parting line separation, a very undesirable situation.

Separation will occur first at B since, in addition to axial tension, bending will tend to take place tending to cause compression at A.

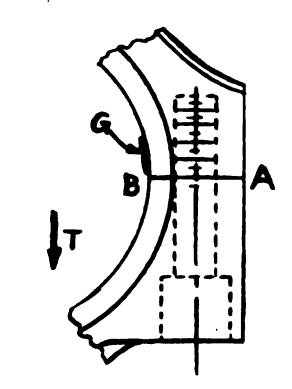


Fig. 12. Parting Line Portion of Connecting Rod

To check for parting line separation, a strain gage was cemented to the inner surface

of the connecting rod bearing boss at G with the bearing cap removed. The gage was then connected to the Anderson Strain Meter and the bridge was balanced. Next the bearing cap was put in place and the screws were tightened. Experience has indicated that a torque of from six to nine pound feet is satisfactory for a 1/4 - 28 cap screw so in this case a torque of eight pound feet was used. This caused the Anderson Strain meter to indicate a compressive strain in the gage at G. Next the maximum anticipated tensile load was applied to the connecting rod assembly. This caused a reduction in the amount of the indicated compressive strain but did not reduce this strain to zero. It was therefore concluded that parting line separation did not occur and an assembly torque of eight pound feet was used for the rest of the testing.

#### BIBLIOGRAPHY

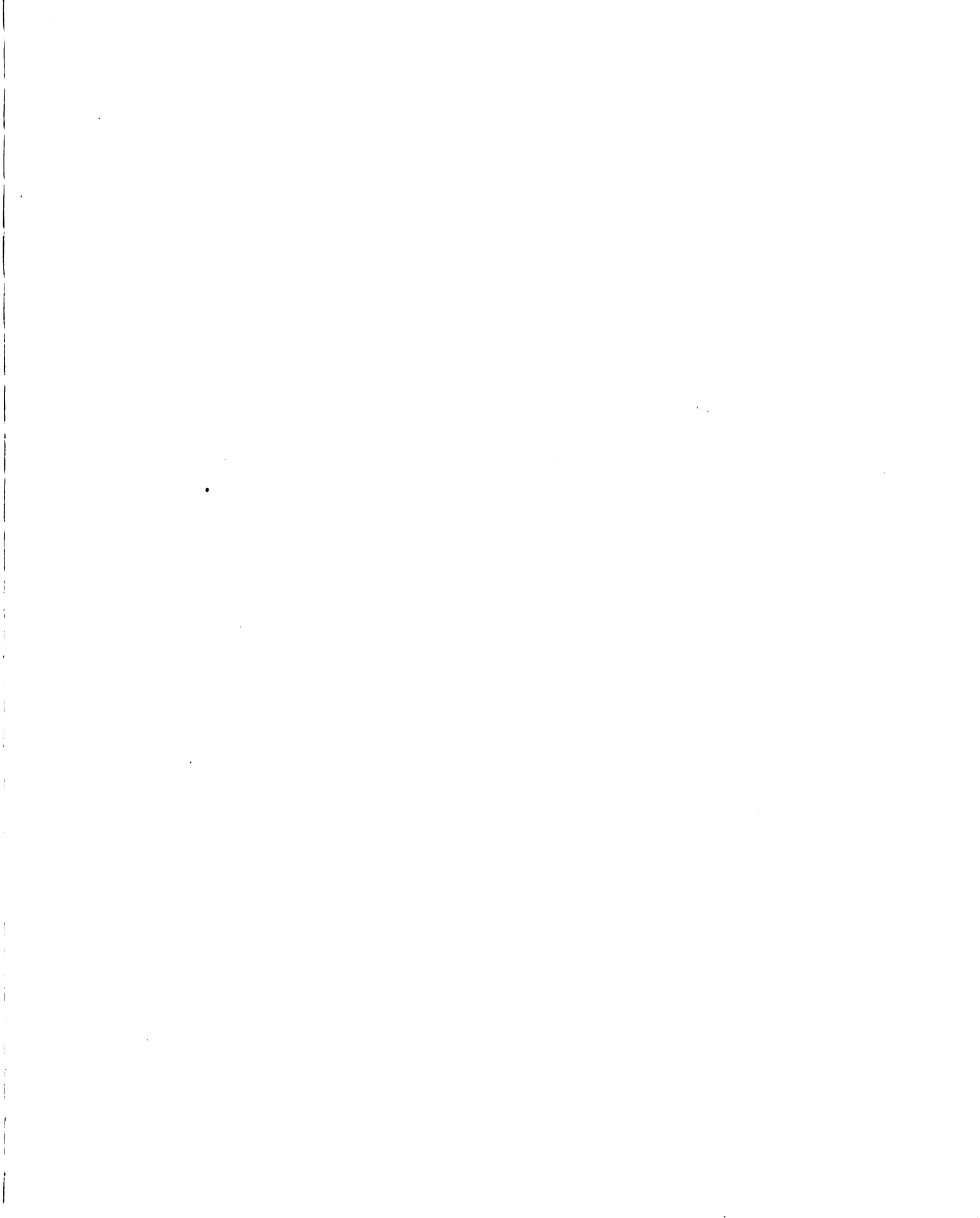
- 1. Diederichs, Herman and Andrae, William C., Experimental Mechanical Megineering, Volume I, John Wiley and Sons, New York, Seventh Printing, 1949, 1082 pp.
- 2. Faires, Virgil Moring, Applied Thermodynamics, Revised Edition, The MacMillan Company, New York, Seventh Frinting, 1950, 460 pp.
- 3. Harris, Charles J., Elementary Engineering Mechanics, Irwin-Farnham, Chicago, 1947, 445 pp.
- 4. Lichty, Lester C., Internal-Combustion Engines, Sixth Edition, McGraw-Hill, New York, 1951, 598 pp.
- 5. Marks, Lionel S., Mechanical Engineers' Handbook, Fifth Edition, McGraw-Hill, New York, Third Impression, 1951, 2236 pp.
- 6. Murphy, Glenn, Advanced Mechanics of Materials, McGraw-Hill, New York, 1946, 307 pp.

1			

# ROOM USE GIVLY

Jan 26 '35

Mar 7 5



MICHIGAN STATE UNIV. LIBRARIES
31293103859595